analytical chemistry

pubs.acs.org/ac Article

Detection of Microplastics in Ambient Particulate Matter Using Raman Spectral Imaging and Chemometric Analysis

Joseph M. Levermore,* Thomas E. L. Smith, Frank J. Kelly, and Stephanie L. Wright

Cite This: *Anal. Chem.* 2020, 92, 8732−8740 Read Online

ACCESS | Metrics & More | Article Recommendations | Supporting Information

ABSTRACT: Microplastics have been observed in indoor and outdoor air. This raises concern for human exposure, especially should they occur in small enough sizes, which if inhaled, reach the central airway and distal lung. As yet, methods for their detection have not spectroscopically verified the chemical composition of microplastics in this size-range. One proposed method is an automated spectroscopic technique, Raman spectral imaging; however, this generates large and complex data sets. This study aims to optimize Raman spectral imaging for the identification of microplastics (≥2 μm) in ambient particulate matter, using different chemometric techniques. We show that Raman spectral images analyzed using chemometric statistical approaches are appropriate for the identification of both virgin and environmental microplastics ≥2 μm in size. On the basis of the sensitivity, we recommend using the developed Pearson's correlation and agglomerative hierarchical cluster analysis for the identification of microplastics in spectral data sets. Finally, we show their applicability by identifying airborne microplastics >4.7 μm in an outdoor particulate matter sample obtained at an urban sampling site in London, United Kingdom. This semiquantitative method will enable the procurement of exposure concentrations of airborne microplastics guiding future toxicological assessments.

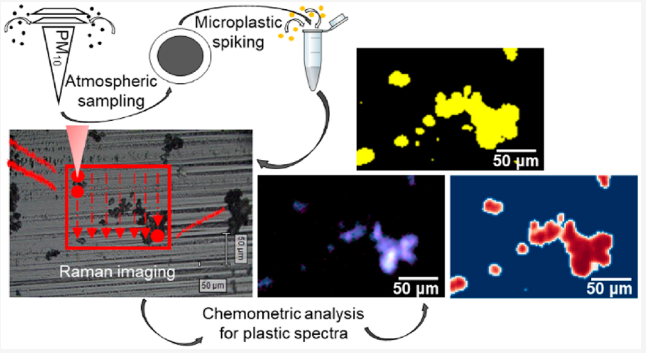

Microplastics, defined here as particulates (0.1−5000 μm maximum dimension) of heavily modified synthetic organic polymers, following recommendations by the European Commission,[1] are ubiquitous in aquatic and terrestrial environments. Recently, their presence in atmospheric particulate matter (PM) has raised concern for population exposure and public health. This is because microplastic inhalation of poly(vinyl chloride) (PVC),[2,3] polyamide (PA),[4] and polyester (PES) dust[5] has been attributed to the onset of occupational lung diseases, albeit at high exposure concentrations ranging from 0.16[6] to 42 mg/m^3.[3]

Aerodynamic diameter is a key property which influences particulate matter (PM) intake via inhalation. Airborne microplastics ≤100 μm aerodynamic diameter (D) are categorized as particulates in the inhalable fraction,[7] the majority being deposited in the nasopharyngeal airway (NPA). Particulate matter ≤10 D (PM_{10}) reach and deposit in the intrathoracic regions of the respiratory system;[8] these particulates are transported via mucociliary clearance, indirectly deposited in the oropharynx, and upon swallowing, will lead to gastrointestinal exposure.[9,10] Particulate matter <2.5 D ($PM_{2.5}$) have the potential to reach the alveolar regions of the lung, where they remain until eliminated by alveolar macrophages or cleared by endocytosis.[11] Hence, airborne microplastics which are <10 D are considered a concern for respiratory health, yet due to methodological challenges in detection, information on their prevalence and concentration is currently limited.

Several studies have reported on airborne microplastics, employing active[12−16] or passive[17−23] sampling methodologies. Given the potential for microplastic misidentification due to overlapping aesthetic, morphological, or fluorescent properties with nonplastic particulates, spectroscopic analysis is an analytical requirement. Of the 12 studies mentioned, 9 spectroscopically verified the composition of suspected microplastics (≥5 μm), using vibrational spectroscopy, that is, Fourier-transform infrared spectroscopy (FTIR), attenuated total reflection-FTIR (ATR-FTIR), or Raman spectroscopy. Typically, researchers in the microplastics field conduct an optical prescreen for suspected airborne microplastics for which a chosen subsample is spectroscopically analyzed.[17−19,21,22] The reliance on putative visual and manual screening of environmental samples for suspected microplastics, typically, constrains analysis to the larger size-fraction

Received: December 2, 2019
Accepted: May 12, 2020
Published: June 22, 2020

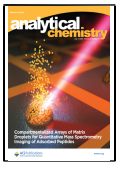

https://dx.doi.org/10.1021/acs.analchem.9b05445
Anal. Chem. 2020, 92, 8732−8740

of suspected microplastics. Larger particulates are easily identified and handled, but this approach is susceptible to operator bias and identifying microplastics in a physiologically relevant size-range (<10 μm) can be challenging, time-consuming, and prone to observer error.

To reduce operator bias, Raman microscopes, have been coupled to particle-finding software to automate particle identification.[24,25] Such software can identify particulates from 300 nm to ≥30 mm, depending on instrument parameters.[26] Nevertheless, its application to air samples is challenging. The high abundance of particulates in ambient samples can result in long analysis durations and, depending on the sample density, under-count particulates contiguous to one another.

Raman spectral imaging (RSI) has been proposed as an alternative approach to combat operator bias and improve spectroscopic analysis of contiguous particulates. Raman microscopes which have successfully used RSI to identify microplastics from 400 nm,[27] in simple spectral images (SIs) containing only the plastic particulate and the Raman substrate, to ≥50 μm, include confocal Raman spectroscopy (CRS), stimulated Raman scattering (SRS[29−31]), coherent anti-Stokes Raman microscopy (CARS[27]), and structured line illumination Raman microscopy (SLI[28]). The advantage of using conventional Raman spectrometers is that they are widely available, intuitive to use and can identify ≥2 μm microplastics. While RSI has the ability to detect virgin microplastics that, if inhaled, would reach the pulmonary alveoli, it has only been validated for the detection of virgin microplastics >4 μm in ambient PM collected on filters.[16] While this technically progressed the limits of microplastic detection, there is still a need to optimize RSI for the identification of respirable airborne microplastics in complex SIs, as $PM_{2.5}$ has been associated with an increased health impact.[32]

The purpose of this study was to develop an automated imaging methodology able to spectroscopically identify airborne microplastics in a physiologically relevant size-range. In doing so, we compare three chemometric techniques for their ability to spectroscopically identify spiked microplastics in a complex PM sample. The predictive chemometric statistics were optimized, applied, and evaluated for their performance to identify both virgin (plastic containing no chemical additives) and environmental microplastics of different sizes and composition. Ultimately, we developed a workflow compatible with a novel air sampler, notably the multivial cyclone sampler (MVCS). The MVCS samples air at a flow rate of 16.5 L/min and, using reverse cyclone technology, collects and retains total suspended airborne PM in Eppendorf vials. The MVCS was identified as an appropriate sampling instrument, as collected samples can be easily prepared for RSI; sample preparation involves the resuspension of collected PM in ethanol (EtOH), and drying of a subsample onto a substrate of optimum composition for RSI. While air samples are the focus in this study, the developed analytical methodology is applicable to a range of sample types given adequate preparation, that is, microplastic purification using density separation or acid digestions. The purified environmental sample can be dried on to a Raman substrate and spectroscopically imaged using RSI. Therefore, RSI coupled to the proposed chemometrics techniques has a broader application beyond air studies.

EXPERIMENTAL SECTION

Reagents and Materials. EtOH was sourced from Fisher Scientific UK (Loughborough, UK). 1, 2, and 10 μm PS microspheres were sourced from Sigma-Aldrich (UK). 4.16 μm PS microspheres were sourced from Spherotech Inc. (Illinois, US). PA, PE, polyethylene terephthalate (PET), polystyrene (PS), polypropylene (PP), and PVC particles were sourced from Goodfellows, Ltd. (UK) (otherwise referred to as virgin plastics). These were all stored as per the supplier recommendations. Environmental plastics of unknown composition were collected opportunistically from a European Beach (Arenal d'en Castell, Menorca) and were cyromilled to reduce their finesse. A total of 50 polycarbonate (PC), PE, PET, PS, PP, and PVC consumer plastics, ranging in physical (i.e., rigidity) and aesthetic characteristics (i.e., color) were obtained from packaging, clothing, and electronic equipment. Black carbon, brake wear debris, diesel, and quartz particulates were gifted from Dr Mudway, King's College London. A Teflo (polytetrafluoroethylene; PTFE; 2.0 μm pore size) filter was sourced from Pall (New York, USA). Sterile disposable scalpel No. 6 blades were sourced from Swan Morton (Sheffield, UK).

Raman Instrumentation Parameters. Raman measurements were performed using Renishaw's inVia Raman Microscope (Renishaw Plc, Wotton-under-Edge, UK), equipped with a 785 nm diode laser. SIs were collected at 19 mW laser power, using the StreamLine scanning mode. The StreamLine function collates spectra for each pixel by line-scanning the Raman laser over an operator defined sample area. Spectral acquisition was conducted using a Lecia microscope via a CFI Plan Fluor ELWD 20×/0.45 and a Lecia N Plan 50×/0.75 objective lens, giving a spatial resolution of 2.6 and 1.1 μm, respectively. The spectral acquisition time for RSI and broad spectra was set to 2 and 10 s per spectra, respectively. The spectrometer's entrance slit of 50 μm combined with a diffraction grating of 600 lines per mm achieved a spectral resolution of 1.9 cm^{-1}. For RSI, spectral acquisition ranged from 924.6 to 1668.0 cm^{-1} Raman shifts (centered at 1300 cm^{-1}), while broad spectra ranged from 200 to 3200 cm^{-1}. At the start of each experiment the spectrometer was calibrated using Renishaw's silicon calibrator. The x and y dimensions of the SI were determined by Renishaw's WiRE software using the laser's spot size and step size between acquisition points.

Substrate Selection. Substrate autofluorescence can be restricted to minimize signal interference by selecting spectroscopically inert Raman substrates.[33] Gold-coated, aluminum foil-covered (otherwise referred to as aluminum slides[34]), stainless steel, low-e, and calcium fluoride (CaF_2) slides were all screened for their signal interference when identifying 1, 2, 4, and 10 μm PS microspheres. For each substrate, three SIs were acquired at random of the dispensed PS microspheres and were analyzed using the chemometric methods, outlined in spectral data analysis section.

Spectral Library. To analyze SIs for the presence of plastic particulates, an in-house plastic spectral library was built. Virgin powders and shavings of consumer plastic samples of PA, PC, PE, PET, PS, PP, and PVC were obtained, deposited on to the chosen Raman substrate, and analyzed without any prior treatment using Raman microscopy. Consumer plastic shavings were obtained using a sterile disposable scalpel to extract small plastic particulates from the edge of the plastics structure. The shavings were obtained or reshaped into sizes

https://dx.doi.org/10.1021/acs.analchem.9b05445
Anal. Chem. 2020, 92, 8732−8740

appropriate for microscopy analysis. For each plastic sample, a SI was acquired from the plastic surface, as well as a broad and narrow spectrum. Pigments are commonly incorporated in consumer plastics and can generate Raman signal that may perturb the identification of the plastic core. Because of this, a pigment commonly incorporated into plastics, copper phthalocyanine (CuPc), was included in the spectral library (Figure S1A[35,36]). The mean spectral fingerprints obtained from the virgin and consumer surface SIs are shown in Figure S1.

Spectral Data Analysis. *Preprocessing.* Spectral alignment was conducted on all Raman spectra using standard normal variance (SNV[37]). Each spectrum was baseline corrected using asymmetrical least-squares baseline correction with lambda (λ) set to 20153.43 and p to 0.0052166 in the multivariate curve resolution-alternating least squares (MCR ALS) program in MATLAB.[38] Spectral smoothing was undertaken using a Savitzky−Golay filter set to a polynomial order of 2 and a frame size of 7 (see the Supporting Information). For cosmic ray removal, Renishaw's Cosmic Ray Remover in Renishaw's WiRE software was used.

To identify plastic associated spectra in the obtained SI, one unsupervised spatial clustering method, Agglomerative Hierarchical Cluster Analysis (AHCA), and two supervised analysis methods, Gaussian Curve Function (otherwise referred to as Gaussian analysis), and Pearson's Correlation Coefficient (PCC), were implemented for comparison.

Agglomerative Hierarchical Cluster Analysis. AHCA is applied to a SI, which has undergone dimensionality reduction using Principal Component Analysis (PCA). PCA projects the original spectra into lower-dimension principal component subspaces.[39] AHCA is a hard-clustering classification model, using the weighted-average-linkage algorithm and a Euclidean distance measure to calculate spectral clustering.[40] AHCA was adapted to a targeted approach for identifying plastic specific spectra using PCC. An r of >0.8 between a cluster's mean spectrum and the spectra in the plastic spectral library confirmed the presence and type of plastic. The cluster locations were converted into a binary image and ascribed a yellow color palette, displaying the presence (yellow) or absence (black) of the mean spectral cluster and particles were counted, outlined in image analysis section.

Gaussian Curve Function. The Gaussian Curve Function is an integral based statistical method, utilizing preselected characteristic Raman bands, indicative of different plastic compositions (Table S1) and aims to identify their presence in a Raman spectral data set (refer to Wright et al.[16]). To ensure the identification of plastic specific Raman bands versus ones referring to chemical additives, Raman band comparisons was completed. Consistent Raman bands between virgin or consumer plastics were ascribed to be of plastic origin and functional group assignment was conducted (Table S1). In SIs of plastic mixtures to improve plastic distinction, plastic specific indicator Raman bands were selected (Table S2). The Gaussian-analyzed SIs were filtered using a Median filter, underwent Raman band thresholding (Table S2), ascribed a Raman band specific color palette (Table S2), and counted as outlined in image analysis section.

Pearson's Correlation Coefficient Analysis. PCC analysis was conducted using an in-house RSI python package, *Polypython*. PCC identifies the linear relationships between spectra in the plastic spectral library (Figure S1) and the unknown spectra contained in a SI (see the Supporting Information). The linear correlation, identified as Pearson's r, between the two variables will range from +1 referring to positive correlations, to −1 indicating a negative correlation and 0 being an independent correlation.[41] For schematic divergence between positive, independent, and negative correlations, the latter are corrected to 0. To ensure false positive results do not occur in multiplastic RSI analysis, a threshold of 0.78r was applied. Particle counts were conducted as outlined in image analysis section.

Image Analysis. Image analysis was conducted in Icy and ImageJ computer programs, to quantify the particle number of identified microplastics in a SI. Image preprocessing of the SIs included a 64-bit raw gray scale image conversion, Gaussian blur filtration with a sigmoid radius of 1.0, a watershed transform,[42] and a Huang thresholder to extract the objects (areas of Raman signal) from the background.[43] Microplastics in the processed SI were counted using an Undecimated Discrete Wavelet Transform (UDWT) detector (see the Supporting Information[44]). Ten simple SI containing individual 2, 4, and 10 μm PS microspheres were imaged using RSI. The SIs were analyzed as per spectral data analysis section, and the area of positive signal was sized in ImageJ. Measurements, referring to pixel number, were acquired in two directions using the line-transect function in ImageJ. The first size measurement was taken along the microsphere's longest axis (Y), and the second was acquired perpendicular to the longest axis (X). The proposed sizing technique is used throughout this investigation. For AHCA and PCC analyzed SI, the pixel number measurements were multiplied by the step size (1.1 and 2.6 μm) to produce micrometer values. For Gaussian analysis the pixel number was multiplied by the Gaussian full width at half-maximum (fwhm) distribution of 2.3555σ (see the Supporting Information). For each size-range the microspheres mean and standard deviation micrometer value is reported in Table S3.

For the PS microsphere spiked PM sample microspheres were sized and categorized as either being 2, 4, or 10 μm based on whether their Y and X values were within the standard deviation of the validation data set (Table S3).

RSI Validation. *Positive Controls.* The most environmentally common microplastics include PE, PP, PS, PA, PVC, and PET (as used in both clothing (polyester) and bottles[45]). To validate the above chemometric techniques for microplastic identification, SIs of virgin PA, PE, PET, PS, PP, and PVC microplastics deposited on an aluminum slide were obtained at random (n = 3).

In the environment, microplastics undergo ultraviolet (UV), mechanical, and biological degradation, which has been shown to impact their unique Raman spectra.[46] To investigate whether environmental degradation impacts microplastic identification, SIs of environmental plastic particulates deposited on an aluminum slide were acquired (n = 3).

Negative Controls. Ambient PM is diverse in composition and commonly includes sea salt, soil dust, inorganic salts (ammonium, nitrate, sodium), trace metals, and organic or elemental carbon,[47,48] all producing their own unique Raman spectra. To understand whether their presence will impact the classification of microplastics, SIs of common environmental PM (black carbon, brake wear debris, diesel, and quartz particulates) and blank EtOH evaporates deposited on to aluminum slides were acquired (n = 3).

Microplastic Spiked Ambient PM Sample Preparation. To validate the proposed method against a representative

https://dx.doi.org/10.1021/acs.analchem.9b05445
Anal. Chem. 2020, 92, 8732−8740

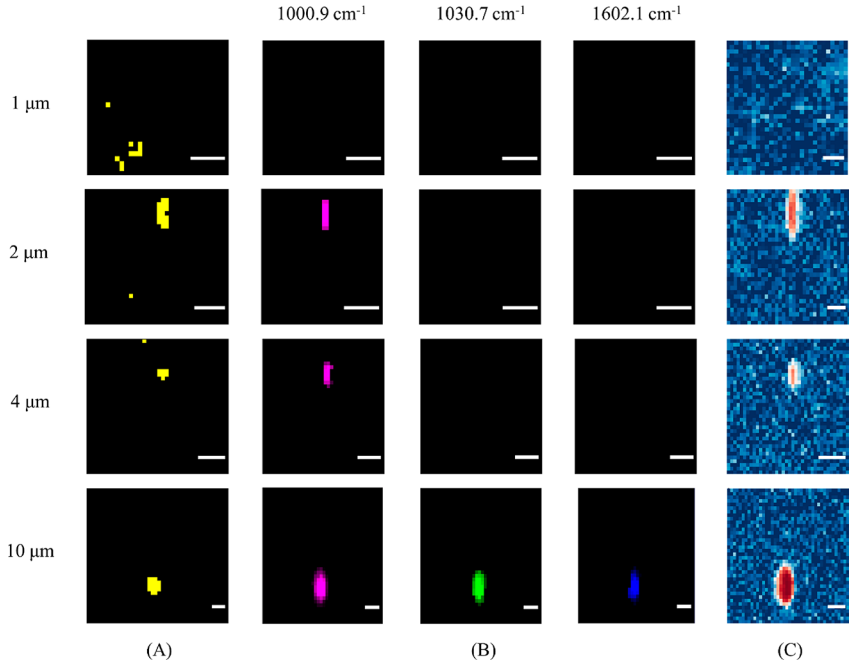

Figure 1. Size-dependent identification of polystyrene (PS) microspheres using Raman spectral imaging. The spectral images (SI) were analyzed using Agglomerative Hierarchal Cluster Analysis (A), Gaussian analysis (B), and Pearson's Correlation Coefficient analysis (C). SIs of 4 and 10 μm PS microspheres were obtained at ∼2.6 μm spatial resolution, and SIs of 1 and 2 μm PS microspheres were acquired at ∼1.1 μm spatial resolution. Yellow (A), magenta, green, and blue (B), and red (C) illustrate the presence of PS's Raman spectrum (A, C) or Raman bands (B). Gaussian-analyzed SI pixel intensities were set to a maximum of 192, 192, and 171 for Raman bands at 1000.9, 1030.4, and 1602 cm^{-1}, respectively. Scale bar: 10 μm.

background a 24-h PM_{10} archived air sample collected from an urban road-side site (Marylebone Road, London, UK) was spiked with PS microspheres of 2, 4, and 10 μm sizes, deposited on an aluminum slide, and analyzed using RSI. The sample was collected onto a Teflo filter using a Partisol Plus 2025 Sequential Ambient Particulate Sampler (flow rate of 16.7 L/min). PM was extracted by submerging the filter in 5 mL of EtOH followed by 5 min of agitation in a sonicating bath at 40 Hz. The extracted PM was dried, weighed, and resuspended in EtOH to a concentration of 312 μg/mL, which corresponds to the mean daily sample weight collected by the desired method of sampling (MVCS) during a spring (2017) sampling campaign. Prior to PS spiking, the PM sample was diluted 1 in 10. A serial dilution was conducted on the 2, 4, and 10 μm PS microsphere stocks and particle number concentrations were determined using a hemocytometer (Table S1). Prior to the aliquoting of 2, 4, and 10 μm PS microspheres, samples were placed in a sonicating bath for 10 s set to 40 Hz to induce a homogeneous distribution. A PS bead mix at a 30 000 ± 5826 n/mL concentration was made, with each microsphere size having a concentration of 10 000 n/mL. The diluted PM sample was spiked with 100 μL of the bead mix, and a 100 μL aliquot was dried dropwise on to an aluminum slide. The drop cast dried in an ellipse shape. The minor and major radius of the micrograph image was measured in ImageJ and the sample area was determined to be ∼21.7 mm^2. SIs were acquired of the entire area at ∼2.6 spatial resolution (Table S4) and 6 randomly chosen subsections were imaged at ∼1.1 μm spatial resolution (Table S5).

An operator-based count was conducted to determine the number of 2, 4, and 10 μm PS microspheres present in the analyzed PS-spiked PM sample drop cast. Using the montage image as a guide, counts were performed at both 20× and 50× magnification thrice by rastering through every field of view from the upper left corner to the lower right corner of the montage image. For every PS microsphere identified by the operator, a photomicrograph was obtained, and size-based analysis was conducted in ImageJ. In addition, spectroscopically identified PS microspheres in the PS-spiked PM sample were also subject to sizing in ImageJ. The operator determined particle number was compared with the SI identification rate using a confusion matrix (Performance Analysis section).

For the randomly acquired SIs at ∼1.1 μm spatial resolution a back calculation was conducted to produce drop-cast wide concentrations of identified 2 μm (AHCA and PCC) and 4 μm (Gaussian) PS microspheres (see the Supporting Information).

The PS spiked PM sample SIs were investigated for the remaining plastics in the in-house plastic's spectral library. All identified particulates were imaged and sized in ImageJ, as per image analysis section, and a broad Raman spectrum was acquired. The broad spectrum was spectroscopically categorized using BioRad's KnowItAll Informatics System − Raman ID Expert (2015) software, using a correlation function as the classifier. Hit quality index (HQI) scores of ≥0.7 were accepted as a correct classification result.[49,50] To visualize the sample wide distribution of RSI identified airborne microplastics a histogram has been used. The bin number for the histogram was determined from the square root of the total microplastic particle number. To determine the sample wide concentration of airborne microplastics in the 24-h PM_{10} sample the spectroscopically identified particulate counts were back-calculated (see the Supporting Information).

Performance Analysis. The suitability of the proposed chemometric techniques (Spectral Data Analysis section) were evaluated and compared, based on their prediction rate, that is, true (type 1 error), and false (type 2 error) observation rates.

https://dx.doi.org/10.1021/acs.analchem.9b05445
Anal. Chem. 2020, 92, 8732−8740

Table 1. Comparison of the Polystyrene Microsphere Count Success Rates for the Different Chemometric Analyses[a]

analysis type	size (μm)	expected particle number	operator identified particle number	operator success rate (%)	SI particle number	SI success rate (%)	recall	F_β score
AHCA	2	93 ± 25	5 ± 4	6 ± 4	21 ± 17	24 ± 18	0.24 ± 0.18	0.36 ± 0.24
	4	100 ± 10	40 ± 22	40 ± 20	75	76 ± 7	0.76 ± 0.08	0.87 ± 0.05
	10	107 ± 23	110 ± 10	85 ± 7	103	90 ± 6	0.94	0.97
	total	300 ± 58	154 ± 37	53 ± 14	199 ± 17	69 ± 11	0.66 ± 0.05	0.80 ± 0.04
Gaussian	2	93 ± 25	5 ± 4	6 ± 4	*	*	*	*
	4	100 ± 10	40 ± 22	40 ± 20	55 ± 48	65 ± 40	0.42 ± 0.39	0.5 ± 0.42
	10	107 ± 23	110 ± 10	85 ± 7	106	92 ± 6	0.96	0.98
	total	300 ± 58	154 ± 37	53 ± 14	161 ± 48	58 ± 19	0.54 ± 0.16	0.70 ± 0.13
PCC	2	93 ± 25	5 ± 4	6 ± 4	42 ± 37	46 ± 34	0.39 ± 0.29	0.50 ± 0.32
	4	100 ± 10	40 ± 22	40 ± 20	93	93 ± 6	0.89 ± 0.04	0.94 ± 0.03
	10	107 ± 23	110 ± 10	85 ± 7	101	88 ± 5	0.92	0.96
	total	300 ± 58	154 ± 37	53 ± 14	236 ± 37	88 ± 20	0.79 ± 0.12	0.87 ± 0.07

[a]The expected count is derived from the known spiking concentrations of 2 and 4 μm microspheres. The manual count refers to an operator-based count using bright field microscopy (for 10 μm PS microspheres only). Spectral image (SI) particle number refers to counts from analyzed SIs. Success rate is expressed as a percent of the expected count. NB: *Identification not achievable.

Ten SIs of an aluminum slide, EtOH evaporates, and 1, 2, 4, and 10 μm PS microspheres deposited on to aluminum slides were obtained at ~2.6 (4 and 10 μm PS microspheres) and ~1.1 μm (1 and 2 μm PS microspheres) spatial resolution. The generated simple SIs, in reference to SIs containing only the Raman substrate and PS microspheres, and SIs of the spiked ambient PM sample were analyzed using the proposed chemometric techniques and their performance was evaluated in a Confusion Matrix using the F_β measure of precision and recall (see the Supporting Information). For confusion matrix analysis of the PS-spiked PM sample, operator determined counts were used for 10 μm PS microspheres. While for 2 and 4 μm PS microspheres RSI was found to outperform operator-based counts; therefore, the RSI detection rate was compared to the expected concentrations.

The proposed chemometric techniques processing speed for classifying SIs of the PS spiked PM sample were recorded. Chemometric analysis was conducted using a Dell OptiPlex 7040 running Windows 10 OS, with an Intel(R) Core i5-6600 CPU @3.30 GHz processor and 32 Gbytes of RAM.

RESULTS AND DISCUSSION

Substrate Validation. Of the SIs obtained of 1, 2, 4, and 10 μm PS microspheres dispensed onto a range of substrates, the low-E slides performed worst due to optical contrast and substrate fluorescence (Figure S2D; limit of detection (LOD) = 10 μm PS microspheres at ~2.6 μm spatial resolution). For the remaining test substrates, although the PS Raman band intensities differed, chemometric analysis spectroscopically identified 2, 4, and 10 μm PS microspheres. The detection of 1 μm PS microspheres was unsuccessful and is attributed to the reduced intensity of bands at 1000 and 1030 cm^{-1}, and the complete suppression of the Raman band at 1602 cm^{-1} (Figures 1 and S3).

The low spectral activity (Figure S2A), ability for identification of microspheres >2 μm (~1.1 μm spatial resolution; Figure 1) and low cost allowing for sample archiving, future reanalysis and/or sample extraction resulted in the selection of aluminum slides as the Raman substrate for the remaining protocol. CaF_2, gold-coated, and stainless steel substrates are relatively expensive, substrate reuse would be necessary to guarantee economic viability.

RSI Validation. *Functional Group Assignment.* Functional group assignment facilitated the identification of plastic associated Raman bands (annotated in Figure S1 and Table S1). CuPc, a pigment commonly incorporated to color plastics, was also distinguishable. A more in-depth investigation into the feasibility of identifying incorporated chemical additives, which if present could impact a plastics Raman spectrum, is needed. This would be useful for understanding microplastic-chemical complexes.[51]

Identification of Virgin and Environmental Microplastics. SIs consisting of a mix of virgin and environmental microplastics, encompassing some of the most environmentally common types, were analyzed using the proposed chemometric techniques. Virgin PA, PE, PET, PS, and PVC microplastics were detected using the evaluated chemometric methods (Figures S4–S6). In SIs of a milled unknown environmental plastic mix, chemometric analysis using the spectral library identified CuPc, PE, PP, and PS particulates (Figures S7–S9). The CuPc particulates are observed to be incorporated in environmental PE and PP particulates, an association previously noted by Dean et al.[52] This confirms RSIs ability to spectroscopically identify virgin and environmental microplastics based on their intrinsic composition, that is, PA, PE, PET, PP, PS, and PVC. Visual inspection of analyzed SIs illustrated PCC analysis is the most competent at identifying microplastics of the smallest size range and particles contiguous to one another compared with Gaussian and AHCA (Figures S4–S9). While the duration and level of photodegradation is unknown, the spectroscopic identification of environmental microplastics in the current study (PE, CuPc, PP, and PS) indicates that this method is suitable for aged particles of a similar composition. However, prolonged UV exposure (1634 days of simulated noon-sunlight) has been observed to modify PVC's Raman spectrum.[46] Thus, it is important to continue to validate analytical methods on aged microplastics and recognize detection limits.

Negative Controls. RSI of black carbon, diesel, break-wear, and quartz particulates, EtOH evaporates, and a blank aluminum slide were analyzed for the presence of plastic related Raman bands or spectra. No false positives results were generated by the chemometric analysis suggesting that the chosen substrate and assessed PM components will not

https://dx.doi.org/10.1021/acs.analchem.9b05445
Anal. Chem. 2020, 92, 8732−8740

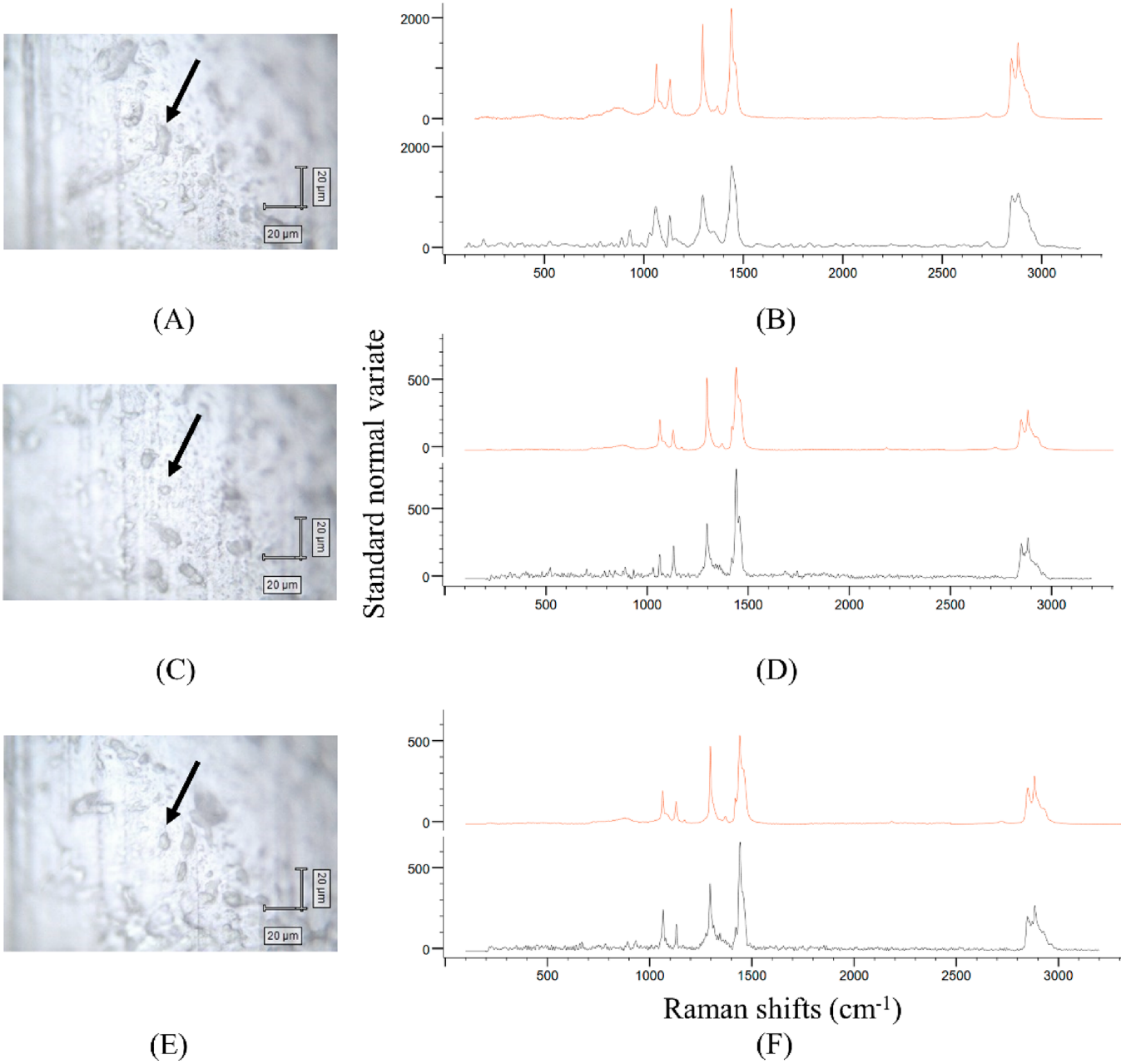

Figure 2. Example of three environmental microplastics identified in the spiked PS ambient sample. Bright field micrographs of the three suspected microplastics, identified by Raman spectral imaging (RSI), were obtained (A, C, E; highlighted by black arrows) and their broad spectra were matched (black) to reference PE-vinyl alcohol (B) and low density-PE (D, F) broad spectra (orange) using BioRad KnowItAll (B, D, F).

interfere with the identification of airborne microplastics Raman spectra (figure not shown).

Identification Rate. The prediction success rate of the different chemometric techniques for 2, 4, and 10 μm PS microspheres in simple SIs is displayed in Table S6. In simple SIs, all three chemometric techniques (AHCA, Gaussian, and PCC) were indistinguishable for 10 μm PS microsphere identification (Table S6). Plastic identification using Gaussian analysis is based on the presence of all selected indicator Raman bands being observed (Figure 1). The relatively weak intensity of Raman bands at 1030 and 1602 cm^{-1} resulted in Gaussian analysis being unable to confirm the presence of 2 and 4 μm PS microspheres in SIs acquired at ~1.1 and ~2.6 μm spatial resolution, respectively. AHCA and PCC identified both microsphere size ranges to an equal extent (Figure 1). For the identification of 2, 4, and 10 μm PS microspheres in simple SI AHCA and PCC performed to a F_β score of 0.83, while the F_β measure score for Gaussian analysis was 0.41.

In SIs containing 1 μm PS microspheres deposited on an aluminum slide, only AHCA was marginally capable of their spectroscopic detection. AHCA identified spectral fingerprints with Raman bands at 1000.9 and 1030 cm^{-1}, albeit at reduced intensities, while the Raman band at 1604 cm^{-1} was completely suppressed (Figure S3). The inclusion of such spectra in the plastic spectral library could result in the identification of 1 μm PS microspheres in SIs obtained at ~1.1 μm spatial resolution. Though, without the Raman band at 1604 cm^{-1}, the potential for false positive errors may increase. Therefore, the identification of 1 μm PS microspheres is

https://dx.doi.org/10.1021/acs.analchem.9b05445
Anal. Chem. 2020, 92, 8732−8740

considered unachievable using the described instrument parameters and chemometric techniques.

The total identification rates of the 2, 4, and 10 μm PS microspheres spiked into the PS spiked PM sample show PCC to perform at the highest success rate (88 ± 20%), recall (0.79), and F_β score (0.70), followed by AHCA and Gaussian function analysis (Table 1). For 10 μm PS microsphere detection, the Gaussian curve function was found to be most effective, followed by AHCA and PCC (Table 1).

For 2 and 4 μm PS microspheres, spectroscopic identification was performed best by PCC analysis, followed by AHCA and Gaussian function analysis (Table 1). Operator-based microscopy identification of 2 and 4 μm PS microspheres was challenging due to their spherical shape, small size, and translucent color resulted in them being easily overlooked and difficult to optically distinguish from ambient particulates at both 20× and 50× magnification. The challenges experienced conducting operator identification of the 2 and 4 μm PS microspheres resulted in the reported count replicates being inconsistent (Table 1). Both, PCC and AHCA techniques show superior identification rates for 2 and 4 μm PS microspheres in comparison to operator determined particle numbers, which failed to detect 94 ± 4% and 60 ± 20% of such PS microspheres, respectively (Table 1). This highlights RSIs enhanced capability for the routine spectroscopic identification of microplastic particulates in the inhalable and respirable size-range and emphasizes the microplastic fields current size-based limitations as operator-based methods persist.

Processing Speed. The proposed chemometric methods were analyzed for their speed at plastic identification in the PS spiked PM sample. The analysis speed for AHCA is dependent on the number of individual components in an RSI, while the speed of Gaussian analysis is determined by the number of analyzed reference peaks. The mean analysis time for the identification of 7 plastics and 1 pigment, across all PS spiked PM sample SIs, was 17 ± 6 min for PCC, 48 ± 5 min via 24 Raman bands for Gaussian analysis, while AHCA took ∼374 ± 395 min via 45 ± 16 separate clusters.

Microplastic Spiked Ambient Sample. All chemometric methods could identify PS microspheres ≥10 μm and all but one (Gaussian) ≥4 μm directly in SIs (∼2.6 μm spatial resolution) of the PS spiked PM sample. At ∼ 1.1 μm spatial resolution the identification of PS microspheres >2 μm in size was achieved for all chemometric methods except the Gaussian function (Figure S10). Though, PCC and AHCA underestimated the number of 2 μm PS microspheres in the PS spiked PM sample by 54 ± 34% and 76 ± 18%, respectively (Table 1). Comparison between the expected and identified microsphere counts in the PS spiked PM sample found PCC to identify 2, 4, and 10 μm PS microspheres at a heightened success rate, recall, and F_β measure, followed by AHCA and last the Gaussian curve function (Table 1). PCC's superior identification rate is attributed to its heightened capacity to differentiate between contiguous microspheres, as AHCA suffers from a spatial amalgamation effect. Watershed algorithms[42] applied to AHCA SIs were unsuccessful in spatially separating contiguous particulates. It is, therefore, necessary to improve the spatial resolution of the imaging function for AHCA to facilitate more accurate microsphere counts. The employed image analysis procedure for the Gaussian function resulted in an unsuccessful or low identification rate for 2 and 4 μm PS microspheres in simple SIs (∼1.1 μm spatial resolution; Table S6); therefore, it is recommended that future chemometric analysis focus on utilizing PCC or AHCA.

Limited access to spectral libraries can restrict spectroscopic identification of environmental microplastics.[22] Therefore, we have developed an online spectral library, which will be available at www.plasticanalytics.com from July 2020. This online library is intended to improve chemical categorization of microplastics in environmental samples, by allowing the research community to upload and download plastic spectra obtained using Fourier transform infrared (FT-IR) and Raman spectroscopy instruments.

Analysis of the PS spiked PM sample using the in-house plastic spectral library resulted in the identification of airborne microplastics, that is, PE (n = 220), PET (n = 1), and PP (n = 2) particles, ranging from 4.7 to 40.9 μm in size in their longest dimension (Figure S11 and Table S7). An example of three of the identified PE particles are shown in Figure 2 and are 16.3 (Figure 2 A), 4.7 (Figure 2 C), and 8.3 μm (Figure 2 E) in size in their longest dimension. Particles were spectroscopically confirmed to be PE-vinyl alcohol (Figure 2A and B) and low density-PE (Figure 2C−F) using BioRad's KnowItAll library. Classification of the suspected microplastics broad Raman spectra using BioRad's KnowItAll library confirmed the proposed chemometric classifications were correct, resulting in no false positive observations. However, with an increased number of environmental particulates scanned, it is expected false positive results will occur; therefore, it is paramount to acquire broad spectra from a subsample of identified microplastics to validate prediction accuracy.

Previous investigations have observed that as microplastic size reduces, concentration increases.[12,13] The same is shown here as 52.5% of the confirmed microplastics were 5−10 μm, 35.0% were 11−20 μm, 2.7% were 21−30 μm, and 0.9% were >31 μm (Figure S11). The reduction in concentration for particles between 5−7.5 μm is hypothesized to be resultant of the reduced Raman signal produced. This reduced Raman signal could be the consequence of surface contaminants being present, that is, biological films or adhered nanoparticles.

The total concentration of airborne microplastics in the 24 h PM_{10} urban road-side sample was 2502 microplastics/m^3. Currently, reported outdoor airborne microplastics range from 5 μm[20] to 2200 μm in length[19] and are predominantly composed of PA, PE, and PP. Here, similarly to current investigations particulates composed of PE, PET, and PP were among the identified airborne microplastic compositions. Studies which have reported on the concentration of airborne microplastics (p/m^3) have observed median concentrations ranging from 0.9 ± 0.6[12] to 2019.0 ± 930.0 microplastics/m^3.[13] The large fluctuation in reported abundance highlights the need for further work to consolidate ambient microplastic concentrations.

Instrument Considerations. RSI offers an automated methodology suitable for the identification of microplastics in the inhalable size range in complex PM samples. In comparison to operator-based optical inspection, RSI removes the potential for operator bias, thereby increasing the likelihood of detecting smaller microplastics. The main limitation of RSI is acquisition time (Tables S4 and S5). To significantly reduce this, restricting sample aliquots to a ≤2 mm area or utilizing modern Raman microscopes, which offer faster mapping capabilities and an improved background fluorescence suppression, is recommended.

https://dx.doi.org/10.1021/acs.analchem.9b05445
Anal. Chem. 2020, 92, 8732−8740

Another vibrational spectroscopy imaging technique commonly employed for the detection of microplastics in environmental samples is FT-IR imaging. Käppler et al.[53] compared RSI and FT-IR imaging based on their ability to identify microplastics in extracted sediment samples (<400 μm sized particulates) concentrated on silicon filters. A 1 × 1 mm area was analyzed using RSI and FT-IR imaging; FT-IR imaging was found to successfully identify microplastics ≥11 μm, while RSI was capable of spectroscopically detecting microplastics ≥5 μm in size.[53] The improved identification of microplastics in a physiologically relevant size range, as achieved by RSI, is paramount for the attainment of robust exposure concentrations. Technological advances in IR imaging instrumentation, that is, atomic force microscope infrared-spectroscopy (AFM-IR), have resulted in successful measurements of nanosized particulates, though this is yet to be demonstrated for microplastics in environmental samples.[54] As FT-IR is a much more time-efficient approach, scanning a 1 × 1 mm area in 20 min in comparison to 38 h for RSI,[53] a methodology integrating FT-IR and RSI could be advantageous. Additionally, environmental samples could be size fractionated at 10 μm; the >10 μm fraction being analyzed using FT-IR and the <10 μm fraction analyzed using RSI.

The presence of biofilms and debris coating the surface of environmental microplastics may generate large amounts of autofluorescence, which could impede the spectral acquisition of the plastic matrix. Therefore, RSI of environmental samples may require further ad-hoc-preprocessing to quench such autofluorescence, for example, by implementing a multipolynomial baseline correction. The development of a multipolynomial fitting function,[55] which iteratively analyses each spectrum in a SI would be highly beneficial and a future development for the *Polypython* package.

This protocol has been developed to be compatible with PM samples collected using the MVCS to enable semiquantitative microplastic analysis: that is, abundance, chemical composition, extrapolated particle number, size distribution, and morphology. In addition to ambient samples, the presented RSI method is likely appropriate to identify microplastics in aquatic, and terrestrial sample types, though adequate sample preprocessing is recommended. Particulates shown to generate plastic signal in the SI should be further optically inspected to conduct morphological analysis (i.e., size, shape, color). Therefore, application of the proposed workflow on MVCS samples, which have been suspended in EtOH, and a subsample is dried dropwise onto a Raman substrate, that is, aluminum slide, will enable the identification of >2 and >4 μm airborne microplastics for RSI acquired at ∼1.1 and ∼2.6 μm spatial resolution, respectively. Moving forward, this workflow could be used in compliment with quantitative techniques, that is, Pyrolysis-Gas Chromatography−Mass Spectrometry (Py-GC-MS) to generate semiquantitative (microplastic abundance (n/m^3), size distribution, chemical composition), and quantitative data sets ($\mu g/m^3$).

CONCLUSION

In conclusion, we have demonstrated that SIs analyzed using Gaussian, AHCA, and PCC chemometric techniques can identify microplastics in the inhalable size-range. In this study, SIs were acquired at ∼1.1 and ∼2.6 μm spatial resolution, which enabled the direct identification of 2, 4, and 10 μm PS microspheres in ambient PM. Investigation for additional plastics in the spectral library identified airborne microplastics composed of PE, PET, and PP at a concentration of 2502 particulates/m^3 at an urban road side site in London, UK. RSI has a clear advantage in removing operator bias, while permitting the identification of airborne microplastics in the inhalable size range, and procurement of microplastic abundance, size distribution, chemical composition, and morphological information. However, it requires long acquisition and data processing times. For the field to progress toward microplastic monitoring in any environmental matrix, more streamlined instrumentation is required. Hence, future work will concentrate on using RSI in compliment with alternative quantitative techniques, such as Py-GC-MS, to generate semiquantitative and quantitative data sets.

ASSOCIATED CONTENT

Supporting Information

The Supporting Information is available free of charge at https://pubs.acs.org/doi/10.1021/acs.analchem.9b05445.

Expanded methodological explanations and additional figures and tables produced to compliment this Article (PDF)

AUTHOR INFORMATION

Corresponding Author

Joseph M. Levermore − *MRC Centre for Environment and Health, Department of Analytical, Environmental and Forensic Sciences, King's College London, London SE1 9NH, United Kingdom;* orcid.org/0000-0002-7815-3467; Email: joseph.levermore@kcl.ac.uk

Authors

Thomas E. L. Smith − *Department of Geography, King's College London, London WC2R 2LS, United Kingdom; Department of Geography and Environment, London School of Economics and Political Science, London WC2A 2AE, United Kingdom*

Frank J. Kelly − *MRC Centre for Environment and Health, Department of Analytical, Environmental and Forensic Sciences, King's College London, London SE1 9NH, United Kingdom*

Stephanie L. Wright − *MRC Centre for Environment and Health, Department of Analytical, Environmental and Forensic Sciences, King's College London, London SE1 9NH, United Kingdom;* orcid.org/0000-0003-1894-2365

Complete contact information is available at: https://pubs.acs.org/10.1021/acs.analchem.9b05445

Notes

The authors declare no competing financial interest.

ACKNOWLEDGMENTS

We would like to thank Mr. Peter Pilecki for technical support with the Raman microscope and Mr. Priyank Shah, Mrs. Basma Qazi Chaudhry, and Professor David Richards for their assistance with chemometric statistical techniques. The Medical Research Council (MRC) Centre for Environment and Health at King's College London (KCL) supported this research (Grant MR/M501712/1). The views expressed are those of the authors and not necessarily those of MRC or KCL.

REFERENCES

(1) European Commission. *Environmental and Health Risks of Microplastic Pollution*, 2019. https://ec.europa.eu/info/publications/

environmental-and-health-risks-microplastic-pollution_en (accessed 2019-12-17).
(2) Szende, B.; Lapis, K.; Nemes, A.; Pinter, A. *Medicina del Lavoro* **1970**, *61* (8), 433−436.
(3) Antti-Poika, M; Nordman, H; Nickels, J; Keskinen, H; Viljanen, A *Thorax* **1986**, *41*, 566−567.
(4) Eschenbacher, W. L.; Kreiss, K.; Lougheed, M. D.; Pransky, G. S.; Day, B.; Castellan, R. M. *Am. J. Respir. Crit. Care Med.* **1999**, *159*, 2003−2008.
(5) Pimentel, J C; Avila, R; Lourenco, A G *Thorax* **1975**, *30*, 204−219.
(6) Lee, H.; Yap, J.; Wang, Y.; Lee, C.; Tan, K.; Poh, S. *Occup. Environ. Med.* **1989**, *46* (11), 820−822.
(7) European Committee for Standardization (CEN). *Workplace Atmospheres—Size Fraction Definitions for Measurement of Airborne Particles*, Report No. BS EN481:1993; CEN, British Standards Institute: London, England, 1993.
(8) Möller, W.; Häußinger, K.; Winkler-Heil, R.; Stahlhofen, W.; Meyer, T.; Hofmann, W.; Heyder, J. *J. Appl. Physiol.* **2004**, *97* (6), 2200−2206.
(9) Foord, N.; Black, A.; Walsh, M. *J. Aerosol Sci.* **1978**, *9* (4), 343−357.
(10) Bohning, D.; Atkins, H.; Cohn, S. *Inhaled Particles V* **1982**, *26* (1−4), 259−271.
(11) Oberdörster, G. *Aerosol Sci. Technol.* **1993**, *18* (3), 279−289.
(12) Dris, R.; Gasperi, J.; Mirande, C.; Mandin, C.; Guerrouache, M.; Langlois, V.; Tassin, B. *Environ. Pollut.* **2017**, *221*, 453−458.
(13) Tunahan Kaya, A.; Yurtsever, M.; Çiftçi Bayraktar, S. *Eur. Phys. J. Plus* **2018**, *133*, 488.
(14) Abbasi, S.; Keshavarzi, B.; Moore, F.; Turner, A.; Kelly, F.; Dominguez, A.; Jaafarzadeh, N. *Environ. Pollut.* **2019**, *244*, 153−164.
(15) Vianello, A.; Jensen, R.; Liu, L.; Vollertsen, J. *Sci. Rep.* **2019**, *9*, 8670.
(16) Wright, S.; Levermore, J.; Kelly, F. *Environ. Sci. Technol.* **2019**, *53* (15), 8947−8956.
(17) Dris, R.; Gasperi, J.; Saad, M.; Mirande, C.; Tassin, B. *Mar. Pollut. Bull.* **2016**, *104* (1−2), 290−293.
(18) Abbasi, S.; Keshavarzi, B.; Moore, F.; Delshab, H.; Soltani, N.; Sorooshian, A. *Environ. Earth Sci.* **2017**, *76* (23), 1−19.
(19) Cai, L.; Wang, J.; Peng, J.; Tan, Z.; Zhan, Z.; Tan, X.; Chen, Q. *Environ. Sci. Pollut. Res.* **2017**, *24* (32), 24928−24935.
(20) Allen, S.; Allen, D.; Phoenix, V.; Le Roux, G.; Durántez Jiménez, P.; Simonneau, A.; Binet, S.; Galop, D. *Nat. Geosci.* **2019**, *12* (5), 339−344.
(21) Klein, M.; Fischer, E. *Sci. Total Environ.* **2019**, *685* (1), 96−103.
(22) Stanton, T.; Johnson, M.; Nathanail, P.; MacNaughtan, W.; Gomes, R. *Sci. Total Environ.* **2019**, *666*, 377−389.
(23) Bergmann, M.; Mützel, S.; Primpke, S.; Tekman, M.; Trachsel, J.; Gerdts, G. *Science Advances* **2019**, *5* (8), eaax1157.
(24) Schymanski, D.; Goldbeck, C.; Humpf, H.; Fürst, P. *Water Res.* **2018**, *129*, 154−162.
(25) Frère, L.; Paul-Pont, I.; Moreau, J.; Soudant, P.; Lambert, C.; Huvet, A.; Rinnert, E. *Mar. Pollut. Bull.* **2016**, *113*, 461−468.
(26) Opilik, L.; Schmid, T.; Zenobi, R. *Annu. Rev. Anal. Chem.* **2013**, *6* (1), 379−398.
(27) Cole, M.; Lindeque, P.; Fileman, E.; Halsband, C.; Goodhead, R.; Moger, J.; Galloway, T. *Environ. Sci. Technol.* **2013**, *47* (12), 6646−6655.
(28) Watanabe, K.; Palonpon, A.; Smith, N.; Chiu, L.; Kasai, A.; Hashimoto, H.; Kawata, S.; Fujita, K. *Nat. Commun.* **2015**, *6* (1), 10095.
(29) Zada, L.; Leslie, H.; Vethaak, A.; Tinnevelt, G.; Jansen, J.; de Boer, J.; Ariese, F. *J. Raman Spectrosc.* **2018**, *49*, 1136−1144.
(30) Cheng, J.; Xie, X. *Coherent Raman Scattering Microscopy*, 1st ed.; Taylor & Francis Group: London, 2013; p 111.
(31) Réhault, J.; Crisafi, F.; Kumar, V.; Ciardi, G.; Marangoni, M.; Cerullo, G.; Polli, D. *Opt. Express* **2015**, *23* (19), 25235.
(32) Pope, C. A., 3rd; Dockery, D. W. *J. Air Waste Manage. Assoc.* **2006**, *56*, 709−742.
(33) Li, W.; Zhao, X.; Yi, Z.; Glushenkov, A.; Kong, L. *Anal. Chim. Acta* **2017**, *984*, 19−41.
(34) Butler, H.; Ashton, L.; Bird, B.; Cinque, G.; Curtis, K.; Dorney, J.; Esmonde-White, K.; Fullwood, N.; Gardner, B.; Martin-Hirsch, P.; Walsh, M.; McAinsh, M.; Stone, N.; Martin, F. *Nat. Protoc.* **2016**, *11* (4), 664−687.
(35) Lewis, P. A. *Organic Colorants, Coloring of Plastics*; John Willey & Sons, Inc., 2005; pp 100−126.
(36) Horton, A.; Svendsen, C.; Williams, R.; Spurgeon, D.; et al. *Mar. Pollut. Bull.* **2017**, *114* (1), 218−226.
(37) Barnes, R.; Dhanoa, M.; Lister, S. *Appl. Spectrosc.* **1989**, *43* (5), 772−777.
(38) Felten, J.; Hall, H.; Jaumot, J.; Tauler, R.; de Juan, A.; Gorzsás, A. *Nat. Protoc.* **2015**, *10* (2), 217−240.
(39) Li, X.; Yang, T.; Li, S.; Wang, D.; Song, Y.; Zhang, S. *Laser Phys.* **2016**, *26* (3), 035702.
(40) Gautam, R.; Vanga, S.; Ariese, F.; Umapathy, S. *EPJ. Techniques and Instrumentation* **2015**, *2*, 8.
(41) Wayne Courtney, E. *Statistics: Correlation Coefficients*, 1st ed.; Amazon Digital Services LLC: USA, 2017; pp 1−17.
(42) Soille, P.; Vincent, L. *Proc. SPIE* **1990**, 240.
(43) Huang, L.; Wang, M. *Pattern Recognition* **1995**, *28* (1), 41−51.
(44) Olivo-Marin, J. *Pattern Recognition* **2002**, *35* (9), 1989−1996.
(45) Smith, M.; Love, D.; Rochman, C.; Neff, R. *Current Environmental Health Reports* **2018**, *5* (3), 375−386.
(46) Lenz, R.; Enders, K.; Stedmon, C.; Mackenzie, D.; Nielsen, T. *Mar. Pollut. Bull.* **2015**, *100* (1), 82−91.
(47) Kundu, S.; Stone, E. *Environ. Sci.: Processes Impacts* **2014**, *16* (6), 1360−1370.
(48) Sýkorová, B.; Kucbel, M.; Raclavský, K. *Perspectives in Science* **2016**, *7*, 369−372.
(49) Karami, A.; Golieskardi, A.; Keong Choo, C.; Larat, V.; Galloway, T. S.; Salamatinia, B. *Sci. Rep.* **2017**, *7*, 1−11.
(50) Kapp, K. J.; Yeatman, E. *Environ. Pollut.* **2018**, *241*, 1082−1090.
(51) Xu, H.; Dinsdale, D.; Nemery, B.; Hoet, P. *Toxicol. Sci.* **2003**, *72* (1), 92−102.
(52) Dean, B.; Corcoran, P.; Helm, P. *J. Great Lakes Res.* **2018**, *44* (5), 1002−1009.
(53) Käppler, A.; Fischer, D.; Oberbeckmann, S.; Schernewski, G.; Labrenz, M.; Eichhorn, K.; Voit, B. *Anal. Bioanal. Chem.* **2016**, *408* (29), 8377−8391.
(54) Dazzi, A.; Prater, C. *Chem. Rev.* **2017**, *117* (7), 5146−5173.
(55) Ghosal, S.; Chen, M.; Wagner, J.; Wang, Z.; Wall, S. *Environ. Pollut.* **2018**, *233*, 1113−1124.

https://dx.doi.org/10.1021/acs.analchem.9b05445
Anal. Chem. 2020, 92, 8732−8740